

# Ruthenium complexes of 2-(2'-pyridyl)benzimidazole as photosensitizers for dye-sensitized solar cells†

Hunan Yi, Joe A. Crayston\* and John T. S. Irvine

School of Chemistry, University of St. Andrews, St. Andrews, Fife, UK KY16 9ST

Received 27th August 2002, Accepted 26th November 2002

First published as an Advance Article on the web 13th January 2003

N-Alkylated carboxylic acid derivatives of 2-(2'-pyridyl)benzimidazole (pbimH) with different chain-lengths (pbim(CH)<sub>n</sub>CO<sub>2</sub>H where *n* = 1–3) and their ruthenium complexes [Ru(bpy)<sub>2</sub>(pbim)](PF<sub>6</sub>)<sub>2</sub> have been synthesized and characterized. 2D COSY and NOESY NMR spectroscopy were used to aid the assignment of the pbim NMR spectrum. The effect of chain-length on the cyclic voltammetry (CV) was studied and the voltammetry of the parent pbimH complex was re-investigated. The ability of the carboxylic acid groups to bind to TiO<sub>2</sub> coated electrodes was confirmed by the observation of a symmetrical, surface-confined Ru<sup>III/II</sup> wave, while the specular reflectance IR revealed a band at 1620 cm<sup>-1</sup> due to the bound carboxylate (COO ··· Ti) group. The efficiencies of solar cells using these sensitizers were rather low, due to the distance between the sensitizer and the surface and the inefficient coupling of the charge-separated excited state to the surface. A fall in the cell open-circuit voltage with chain length reflected this distance effect. Time-resolved luminescence spectroscopy indicated that rapid electron injection into the TiO<sub>2</sub> conduction band was occurring (<30 ns), but this is not fast enough to compete effectively with alternative excited state processes.

## Introduction

In the last decade, an order of magnitude increase in solar energy conversion efficiencies at dye-sensitized photoelectrochemical cells has been realized by attaching ruthenium polypyridyl complexes to high surface area TiO<sub>2</sub> electrodes.<sup>1</sup> This discovery has provoked many research studies, which have been reviewed extensively.<sup>2–11</sup> The currently accepted mode of working of the cell is shown in Fig. 1. After light absorption by the

field and flows through an external cell to perform useful work. The back-reaction (rate constant, *k*<sub>er1</sub>) is unproductive and should be minimised. Most cells have high efficiency as *k*<sub>er1</sub> ≪ *k*<sub>inj</sub>. The oxidized dye is reduced by an electron donor (I<sup>-</sup>) present in the electrolyte (*k*<sub>2</sub>). Reduction of the oxidized donor (I<sub>3</sub><sup>-</sup>) occurs at the counter electrode and the solar cell is therefore regenerative. A variety of sensitizers has been reported to date, yet still the most efficient and stable ones are based on Ru(II) polypyridyl coordination compounds.<sup>1,9,12,13</sup> In particular, the benchmark complex RuN<sub>3</sub>, **1**, has attracted the most attention.<sup>1</sup>

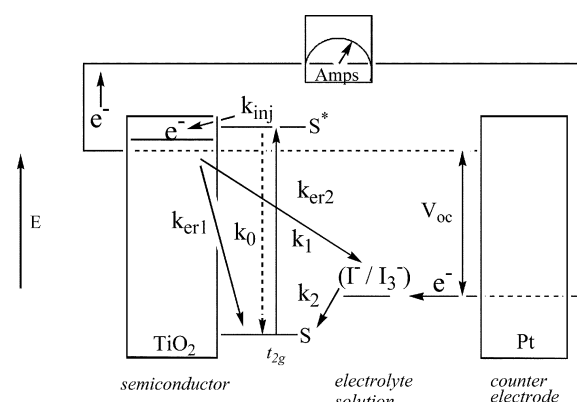
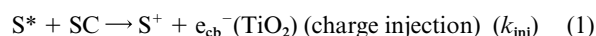
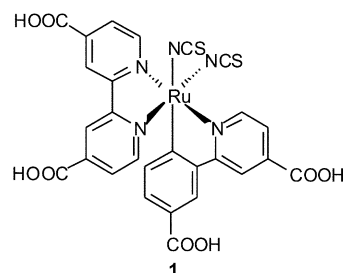


**Fig. 1** Schematic representation of electron transitions in a dye-sensitized solar cell. *k*<sub>0</sub> = rate constant for decay of excited state (S\* → S); *k*<sub>inj</sub> = rate constant for electron injection into TiO<sub>2</sub> (S\* → e<sup>-</sup><sub>TiO<sub>2</sub></sub>); *k*<sub>er1</sub> = rate constant for electron recombination with oxidized dye (e<sup>-</sup> + S<sup>+</sup>); *k*<sub>er2</sub> = rate constant for electron recombination with redox mediator (e<sup>-</sup> + I<sub>3</sub><sup>-</sup>).

dye the excited dye can decay to the ground state radiatively or non-radiatively (with rate constant *k*<sub>0</sub>) or inject an electron into the semiconductor conduction and become oxidized:



Charge injection can happen in less than 1 ps. The electron is then swept to the semiconductor bulk by the surface electric

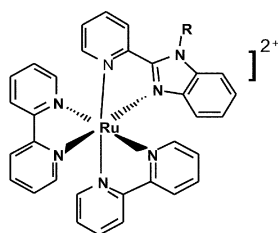


This compound possesses metal-to-ligand charge transfer (MLCT) absorption bands that harvest a large fraction of visible light. It was the most efficient sensitizer until [Ru(tcterpy)-(SCN)<sub>2</sub>]SCN (tcterpy = 4,4',4''-tricarboxy-2,2':6'',2'-terpyridine) was reported.<sup>14</sup> The dye should have an anchoring group such as silanyl, carboxyl and phosphonato which reacts spontaneously with surface hydroxyl groups of oxide surfaces to form ester linkages that exhibit good stability. The aim of our work is to improve the efficiency of dye-sensitized solar cells by designing new sensitizer molecules and by improving the TiO<sub>2</sub>-sensitizer interaction. There are many requirements for the dye, some conflicting.<sup>2</sup> In addition to low cost and high stability in the oxidized, ground, and excited states there are the following requirements: (1) an excited state π\* level that lies at higher energy (*i.e.* more negative potential) than the semiconductor conduction band edge; (2) a positive ground state Ru<sup>3+/2+</sup>-oxidation potential to ensure rapid oxidation by the I<sub>3</sub><sup>-</sup> donor; and (3) intense absorption in the solar region, accompanied by formation of the excited state upon light absorption, regardless of the excitation wavelength. One method of moving λ<sub>max</sub> to longer wavelength is to make *E*(Ru<sup>3+/2+</sup>) less positive (use good π donor ligands to raise the t<sub>2g</sub> level), but this will tend to slow down the reaction with donor (point (2) above). The ligand π\* level can

† Electronic supplementary information (ESI) available: details of the luminescence measurements and solar cell construction and testing; synthesis details; <sup>1</sup>H-<sup>1</sup>H COSY and NOESY 2D spectra for [(bpy)<sub>2</sub>Ru(pbimH)](PF<sub>6</sub>)<sub>2</sub>. See <http://www.rsc.org/suppdata/dt/b2/b208289f/>

also be lowered by adding substituents. However, too low a level would inhibit electron injection into the conduction band (point 1)). Finally, to make the absorption bands more intense, extended ligands with phenyl group substituents may be used in order to increase the transition dipole moment.

Another factor that may be important is the distance between the anchoring group and the semiconductor. A particular advantage of interfacial charge-separated states at semiconductor materials is that the injected electron can be collected as an electrical response. This forms the basis for new applications that exploit both the electronic and optical properties of the sensitized materials, such as charge storage, displays, chemical sensing and optical switching. To achieve a charge-separated state to improve the efficiency of energy transfer, some work has been done on slowing down the charge recombination process. One strategy is to increase charge-separation lifetimes by exploring the performance of a more complex molecular sensitizer Ru(dcpyl)<sub>2</sub>(bpy-PTZ), with a covalently bound electron donor phenothiazine (PTZ) to quench the Ru<sup>3+</sup> hole formed after charge injection.<sup>15</sup> This transfers the hole farther away from the TiO<sub>2</sub> surface in order to reduce the likelihood of back electron transfer. Another strategy is that the distance between the semiconductor electrode and the dye-sensitizer can be optimized by introducing a bridging group between them, *i.e.* -CH<sub>2</sub>, or -C<sub>6</sub>H<sub>4</sub>. In such a way, a charge separated state can also be achieved after an electron is injected from the donor to the acceptor. Thus, we are developing a series of ruthenium polypyridyl complexes with anchoring groups of different chain-length (**2a-d**).



**2a-d**; R=H, (CH<sub>2</sub>)<sub>n</sub>COOH; n = 1-3  
[Ru(bpy)<sub>2</sub>(L)]<sup>2+</sup>; L = L<sub>1</sub>, L<sub>2-4</sub>

In this way, we can find a reasonable chain-length connecting the Ru complex to the TiO<sub>2</sub> nanocrystalline electrode surface to see if there is an optimum distance which minimizes back electron transfer without sacrificing a high rate of charge injection. The pbim ligand possesses an NH group which can be deprotonated and derivatised.<sup>16,17</sup> The alkylated pbim ligand features in a number of mixed-ligand Ru sensitizer complexes.<sup>18-20</sup> Alkylation of pbim with pendant carboxylic acid groups of different spacer lengths is our proposed way to adjust the distance between the semiconductor and the dye-sensitizer to find the optimum distance.

## Experimental

### Chemicals and materials

RuCl<sub>3</sub>·3H<sub>2</sub>O (Aldrich), 2-(2'-pyridyl)benzimidazole (Aldrich), 2,2'-bipyridine (Aldrich), ethyl bromoacetate (Aldrich), ethyl acrylate (Fluka), ethyl bromobutylate, butyllithium (Aldrich), tetra-*n*-butylammonium hexafluorophosphate (Fluka, electrochemical grade) and DMF (Aldrich) were used as received. THF was refluxed from potassium.

### Measurements

Cyclic voltammograms was recorded using an EG and G PARC 273 A potentiostat/galvanostat controlled by version 4.11 of the Electrochemistry Research Software running on a PC. All the experiments were carried out in degassed HPLC grade

acetonitrile solution containing ruthenium complexes (5 × 10<sup>-4</sup> M) and TBAP (0.1 M) as a supporting electrolyte. Measurements were carried out using a saturated calomel electrode (SCE) as the reference with a Luggin capillary and a Pt wire as the counter electrode. The reference electrode, separated from the voltammetric cell by a salt bridge, was Ag/AgNO<sub>3</sub> (0.01 M in CH<sub>3</sub>CN). The electronic spectrum was recorded on a Perkin-Elmer spectrometer Lambda 14P spectrophotometer. Details of the luminescence measurements and solar cell construction and testing may be found in the ESI. †

### Ligand preparations

A representative procedure is given here, see the ESI for a full listing.

**Ethyl(2-pyridin-2-yl-benzimidazol-1-yl)acetate L<sub>2</sub>'.** *Method A.* To a suspension of 2-(2'-pyridyl)benzimidazole (2 g, 10.2 mmol) in 10 ml DMF was added Cs<sub>2</sub>CO<sub>3</sub> (0.33 g, 1 mmol) and K<sub>2</sub>CO<sub>3</sub> (1.41 g, 10.2 mmol). After stirring for 5 min, ethyl bromoacetate (1.30 ml, 11.5 mmol) was added dropwise. The mixture was stirred for 24 h and then evaporated to dryness. The residue was extracted with ethyl acetate (100 ml) and then washed with water (3 × 30 ml) and brine (3 × 30 ml), dried in anhydrous Na<sub>2</sub>SO<sub>4</sub> overnight and the solvent was evaporated. The product was recrystallized from ethyl acetate-hexane to afford the product (1.5 g, 52%).

*Method B.* 2-(2'-Pyridyl)benzimidazole (2 g, 10.2 mmol) was dissolved in 20 ml anhydrous THF under N<sub>2</sub>. The solution was cooled to -78 °C and butyllithium (4.5 ml × 2.5 mol L<sup>-1</sup>, 11.0 mmol) was added with stirring. After addition, the mixture was kept at -78 °C for 3 h and then ethyl bromoacetate (1.30 ml, 11.5 mmol) was added dropwise. It was allowed to warm to room temperature and then refluxed for 3 h under anhydrous conditions. The mixture was poured into 50 ml water and extracted with ethyl acetate (3 × 50 ml). The organic phase was washed with water (3 × 30 ml) and brine (3 × 30 ml), dried in anhydrous Na<sub>2</sub>SO<sub>4</sub> overnight and the solvent was evaporated. The product was recrystallized from ethyl acetate-hexane (2.0 g, 70%). <sup>1</sup>H NMR (CDCl<sub>3</sub>) δ 9.34 (d, 1 H), 8.74 (d, 1 H), 8.31 (t, 1 H), 8.12 (t, 1 H), 7.6 (m, 4 H), 5.78 (s, 2 H), 4.22 (q, 2 H), 1.21 (t, 3 H). Anal. calc. for C<sub>14</sub>H<sub>11</sub>N<sub>3</sub>O<sub>2</sub>: C, 68.33; H, 5.34; N, 14.94. Found: C, 68.34; H, 5.57; N, 14.92%.

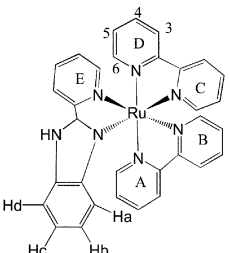
### Synthesis of complexes

More details are available as ESI.

**[Ru(bpy)<sub>2</sub>(L<sub>1</sub>)](PF<sub>6</sub>)<sub>2</sub> (**2a**) (L<sub>1</sub> = pbimH).** Ru(bpy)<sub>2</sub>Cl<sub>2</sub>·H<sub>2</sub>O (1.0 g, 1.9 mmol) and 2-(2'-pyridyl)benzimidazole (0.37 g, 1.9 mmol) were dissolved in 25 ml ethanol and refluxed for 4 h under argon. After reaction, the solution was cooled to room temperature and excess KPF<sub>6</sub> aqueous solution was added. The precipitate was collected by filtration and the crude product was recrystallized from methanol-acetone (1.64 g, 95%).<sup>5</sup> UV-Vis (λ<sub>max</sub>) 460 nm (ε = 7500 M<sup>-1</sup> cm<sup>-1</sup>). <sup>1</sup>H NMR (DMSO-*d*<sub>6</sub>) δ 8.95 (t, 3 H), 8.87 (d, 1 H), 8.72 (d, 1 H), 8.39 (t, 2 H), 8.28 (p, 2 H), 8.22 (t, 1 H), 8.10 (d, 1 H), 7.98 (d, 1 H), 7.95 (d, 1 H), 7.92 (d, 2 H), 7.88 (d, 1 H), 7.73 (t, 1 H), 7.67 (br, 3 H), 7.62 (t, 1 H), 7.52 (t, 1 H), 7.19 (t, 1 H), 5.82 (d, 1 H). Anal. calc. for C<sub>32</sub>H<sub>25</sub>F<sub>12</sub>N<sub>7</sub>P<sub>2</sub>: C, 42.77; H, 2.78; N, 10.91. Found: C, 42.79; H, 2.25; N, 10.73%.

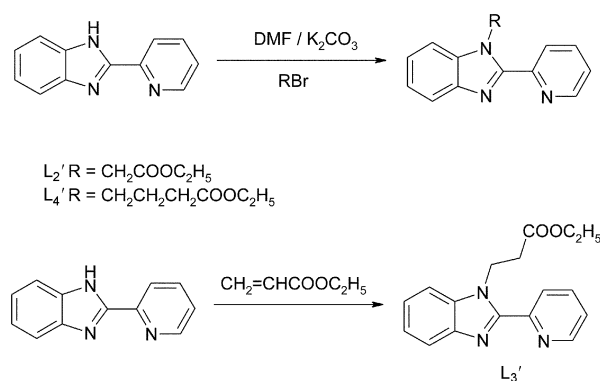
**[Ru(bpy)<sub>2</sub>(L<sub>2</sub>)](PF<sub>6</sub>)<sub>2</sub> (**2b**) (L<sub>2</sub> = pbimCH<sub>2</sub>CO<sub>2</sub>H).** This was prepared by following the same procedure as that for the preparation of [(bpy)<sub>2</sub>Ru(pbimH)](PF<sub>6</sub>)<sub>2</sub> except that pbimCH<sub>2</sub>CO<sub>2</sub>H was used as the starting material, 93% yield. <sup>1</sup>H NMR (DMSO-*d*<sub>6</sub>) δ 8.85 (t, 3 H), 8.76 (d, 1 H), 8.46 (d, 1 H), 8.22 (t, 1 H), 8.10 (br, 4 H), 7.97 (d, 1 H), 7.91 (d, 1 H), 7.82 (d, 1 H), 7.72 (br, 3 H), 7.48 (br, 6 H), 7.17 (t, 1 H), 5.68 (t, 1 H), 5.56 (s, 2 H). Anal. calc. for RuC<sub>34</sub>H<sub>27</sub>F<sub>12</sub>N<sub>7</sub>O<sub>2</sub>P<sub>2</sub>: C, 42.69; H, 2.84; N, 10.25. Found: C, 42.78; H, 2.60; N, 10.66%.

**Table 1**  $^1\text{H}$  chemical shift assignment ( $\delta$ ) of  $[(\text{bpy})_2\text{Ru}(\text{pbimH})](\text{PF}_6)_2$  in  $\text{DMSO}-d_6$ 

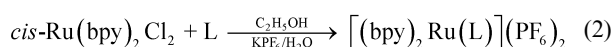
	H3	H4	H6	H5	Benzene
	8.85 ( $\text{H}_{\text{B3}}$ , $\text{H}_{\text{A3}}$ , $\text{H}_{\text{D3}}$ ), 8.75 (d, $\text{H}_{\text{C3}}$ ), 8.59 (d, $\text{H}_{\text{E3}}$ )	8.25 ( $\text{H}_{\text{E4}}$ , $\text{H}_{\text{B4}}$ ), 8.14 ( $\text{H}_{\text{A4}}$ , $\text{H}_{\text{D4}}$ ), 8.09 (t, $\text{H}_{\text{C4}}$ )	7.96 (d, $\text{H}_{\text{B6}}$ ), 7.84 (d, $\text{H}_{\text{C6}}$ ), 7.82 (d, $\text{H}_{\text{D6}}$ ), 7.78 ( $\text{H}_{\text{A6}}$ , $\text{H}_{\text{d}}$ ), 7.73 (d, $\text{H}_{\text{E6}}$ )	7.60 (t, $\text{H}_{\text{B5}}$ ), 7.53 ( $\text{H}_{\text{E5}}$ , $\text{H}_{\text{A5}}$ , $\text{H}_{\text{C5}}$ ), 7.49 (t, $\text{H}_{\text{D5}}$ ),	7.40 (t, $\text{H}_{\text{c}}$ ), 7.08 (t, $\text{H}_{\text{b}}$ ), 5.68 (d, $\text{H}_{\text{a}}$ )

## Results

The synthesis of the carboxylic acid derivatives of pyridylbenzimidazole was hampered by the unreactivity of the NH group ( $\text{p}K_{\text{a}}$  ca. 14 for parent benzimidazole)<sup>21</sup> and the possibility of pyridine quaternization. After deprotonation double alkylation of the benzimidazole ring is prevented as otherwise the aromaticity of the five-membered ring would be lost.<sup>22</sup> There seemed to be no obvious and established route to the missing member of the series,  $\text{pbimCO}_2\text{H}$ , save for reaction with ethyl chloroformate.<sup>23</sup> However, this failed because when hydrolysed from its ester form, decarboxylation occurred. Reactions to produce the other members of the series were carried out in DMF solution with potassium carbonate as the base, in which the bromo-substituted ester starting material was at risk of being hydrolysed. Nevertheless, the reaction was successful in all cases except for the synthesis of  $\text{pbim}(\text{CH}_2)_2\text{CO}_2\text{Et}$  ( $\text{L}_3'$ ). A possible explanation is that the desired  $\text{S}_{\text{N}}2$  reaction is competitive with the elimination reaction to give ethyl acrylate under strongly basic conditions. It might be easier to carry out the deprotonation after complexation, since the  $\text{p}K_{\text{a}}$  falls to ca. 6.8<sup>24</sup> but this was not attempted. Instead, this ligand was prepared by reacting 2-(2'-pyridyl)benzimidazole with ethyl acrylate in a Michael addition reaction with 1,3,4,6,7,8-hexahydro-2H-pyrimido[1,2-a]pyrimidine as the catalyst (Scheme 1).



It was decided to use the acid form, rather than the ester, to anchor the complex to the  $\text{TiO}_2$  surface. Although the  $\text{TiO}_2$  surface is capable of catalyzing the hydrolysis of esters, IR evidence indicates that only partial hydrolysis occurs,<sup>25</sup> and some loss of solar cell efficiency has been noticed using the ester rather than the acid.<sup>26</sup> Attempts to make the homoleptic  $[\text{Ru}(\text{L})_3]^{2+}$  complexes were unsuccessful starting from  $\text{RuCl}_3$ , using the method for  $\text{pbimH}$ , presumably due to the potential for the ligands to bind *via* the oxygen of the carboxylate group. Instead, the ligands were reacted with *cis*- $[\text{Ru}(\text{bpy})_2\text{Cl}_2]^{2+}$  and purified using published methods:<sup>27</sup>



Isolation of the mono-substituted products was achieved by addition of an aqueous solution of  $\text{KPF}_6$  to the reaction mixture. Purification of the crude products was accomplished in most cases by recrystallization from dry methanol-acetone. The final products tend to be insoluble in most solvents including water, but dissolve well in acetone.

## NMR Spectroscopy of the pbim complex

The  $^1\text{H}$  NMR spectrum of  $[(\text{bpy})_2\text{Ru}(\text{pbimH})](\text{PF}_6)_2$  in  $\text{DMSO}-d_6$  is shown in Fig. 2. The chemical shift assignment of the

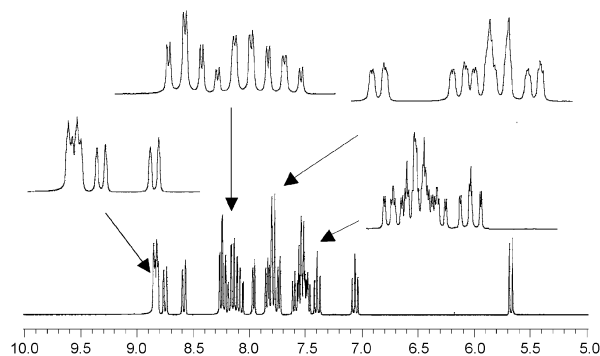


**Fig. 2**  $^1\text{H}$  NMR of the  $\text{L}_1$  complex  $[(\text{bpy})_2\text{Ru}(\text{pbimH})](\text{PF}_6)_2$  in  $\text{DMSO}-d_6$  (below) and with expanded regions of the pyridyl protons (above).

protons of the  $\text{L}_1$  complex  $(\text{bpy})_2\text{Ru}(\text{pbimH})(\text{PF}_6)_2$  is listed in Table 1. The assignment of the chemical shift of the protons was determined by  $^1\text{H}-^1\text{H}$  COSY and NOESY 2D spectroscopy (see ESI). The correlation of each proton was observed in the  $^1\text{H}-^1\text{H}$  COSY spectrum, which distinguishes the protons in different positions (H3, H4, H5, H6) on different pyridine rings (A, B, C, D, E) as defined in the structure in Table 1.

The chemical shifts of the protons on the pbim benzene rings, however, separate at higher field, especially  $\text{H}_{\text{a}}$  at 5.68 ppm because of the ring current effect with the benzene ring facing pyridine A in the complex. First of all, we can determine the chemical shift of the protons on the benzene ring of  $\text{pbimH}$  since they are far apart from other protons from the COSY spectrum.  $\text{H}_{\text{a}}$  is upshifted at 5.68 ppm because of the ring current we mentioned earlier which arises when  $\text{pbimH}$  is coordinated to the ruthenium center. By reading across to the left (or down) from the  $\text{H}_{\text{a}}$  (5.68 ppm) peak in the COSY spectrum, we can immediately assign  $\text{H}_{\text{b}}$ ,  $\text{H}_{\text{c}}$  and  $\text{H}_{\text{d}}$  peaks. The chemical shifts of the bipyridine protons separate in groups as H3, H4, H6 and H5, and each group contains the protons from the bipyridine rings and the pyridine ring from  $\text{pbimH}$ . Bipyridine H3 and H3' coupling was observed in the NOESY spectrum, which holds a key to the assignments of the rest of the protons by walking around the pyridine rings from the COSY spectrum. The only H3 signal ( $\delta$  8.70, measured in MeCN) without a cross peak must be  $\text{H}_{\text{E3}}$ , so from the COSY spectrum we can

**Table 2** Data from UV absorption and emission spectra of the  $[(bpy)_2Ru(pbimH)](PF_6)_2$  complex and its derivatives measured in  $CH_3CN$ 

Compound	$\lambda_{max}/nm$ ( $\epsilon/M^{-1} cm^{-1}$ )	Emission/nm (free solution)	Emission/nm (on $TiO_2$ )
$[(bpy)_2Ru(pbimH)](PF_6)_2$	242 (22400), 285 (42800), 315 (17200), 431 (sh), 455 (8400)	653	—
$[(bpy)_2Ru(pbimC_2)](PF_6)_2$	243 (21600), 287 (45200), 315 (18400), 432 (sh), 458 (9600)	662	643
$[(bpy)_2Ru(pbimC_3)](PF_6)_2$	243 (22500), 283 (46500), 314 (18800), 431 (sh), 457 (15400)	661	648
$[(bpy)_2Ru(pbimC_4)](PF_6)_2$	240 (28000), 280 (48800), 315 (19200), 431 (sh), 457 (10600)	653	647

Note:  $pbimH = L_1$ ,  $pbimC_2 = L_2$ ,  $pbimC_3 = L_3$ ,  $pbimC_4 = L_4$ .

determine all the E ring proton assignments. The unique signal at  $\delta$  8.87 must correspond to the unique pyridine ring C *trans* to the benzimidazole group. Then we can use the COSY to assign all the C and D protons. A similar process yields A and B assignments.

### Electronic absorption spectra

Data from the absorption spectra for the complexes obtained in acetonitrile in the visible region are summarized in Table 2. The low energy absorption band at about  $\lambda_{max} = 455$  nm could be assigned to the  $\pi^*$  (bpy)  $\leftarrow d\pi$  (Ru) metal-to-ligand charge transfer transition. The higher energy bands, 240 and 285, 315 nm, are the pyridylbenzimidazole and bipyridyl intraligand  $\pi-\pi^*$  transitions respectively. The visible absorption band of the pbim complex is blue-shifted relative to that of  $[Ru(dcpv)_2(SCN)_2]$  ( $\lambda_{max} = 537$  nm). The absorption spectrum of the pbimH complex  $[(bpy)_2Ru(L_1)](PF_6)_2$  is shown in Fig. 3.

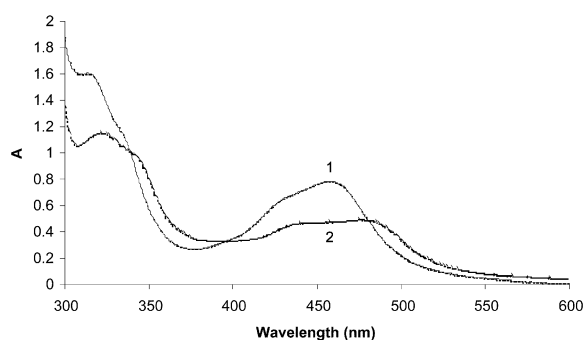


**Fig. 3** Absorption spectra of  $[(bpy)_2Ru(L_1)](PF_6)_2$  in ethanol- $H_2O$  (20 : 1) in the absence (1) and in the presence (2) of NaOH (mole ratio to the complex = 2 : 1) at 25 °C.

When 100  $\mu$ l of 0.01 M NaOH was introduced into the solution, as shown below, the shoulder at 315 nm became a full peak at 325 nm (Fig. 3), indicating that the concentration of the deprotonated form of pbimH increased. The peak position at 455 nm in the visible light region decreased while a new peak at 440 nm started to take shape, however, leading to lower energy shifts of the absorption maxima on deprotonation of the coordinated pbimH ligand. Similar phenomena were observed by Haga<sup>24</sup> when pimH (2-(2'-pyridyl)imidazole) and biimH (2,2'-biimidazole) were used as the coordinating ligands upon deprotonation. Data from the luminescence spectra of  $[(bpy)_2Ru(pbimH)](PF_6)_2$  and its alkylated derivatives are shown in Table 2. The emission maxima are almost identical, near 660 nm in free solution and about 645 nm adsorbed on a  $TiO_2$  film, when excited at 400 nm at room temperature (Fig. 4)

### Electrochemistry

The data for the oxidation of the pbim complexes are summarized in Table 3. The cyclic voltammogram of the oxidation of  $[(bpy)_2Ru(pbimC_2)](PF_6)_2$  in MeCN is shown in Fig. 5, with ferrocene added as the potential calibrator. The effect of N-alkylation of pbim complexes on the  $Ru^{3+/2+}$  shows that the tendency of the pbim complexes to be oxidized at the elec-

**Table 3** Voltammetric data obtained for the oxidation of ruthenium 2-(2'-pyridyl)benzimidazole complexes (1 mM) in acetonitrile at a platinum electrode. The scan rate was at 100  $mV s^{-1}$ . Potential referenced to added ferrocene ( $\Delta E_p = 78$  mV)

Compound	$E_p^{ox}/mV$	$E_p^{red}/mV$	$E_{1/2}/mV$
$[(bpy)_2Ru(pbimH)](PF_6)_2$	825	747	786
$[(bpy)_2Ru(pbimC_2)](PF_6)_2$	848	768	808
$[(bpy)_2Ru(pbimC_3)](PF_6)_2$	820	746	783
$[(bpy)_2Ru(pbimC_4)](PF_6)_2$	809	733	771

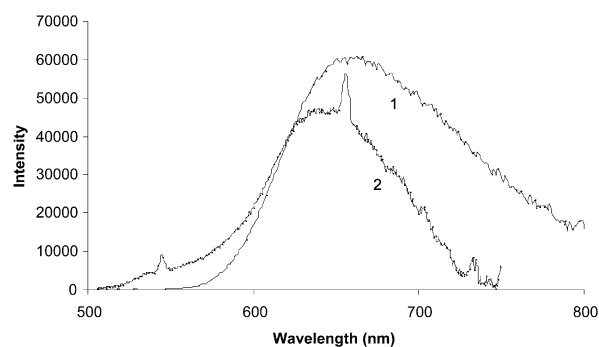


**Fig. 4** Emission spectra of  $[(bpy)_2Ru(pbimC_2)](PF_6)_2$  ( $5 \times 10^{-5}$  M) in MeCN at  $T = 298$  K when excited at 400 nm, (1) free solution and (2) adsorbed on  $TiO_2$ .

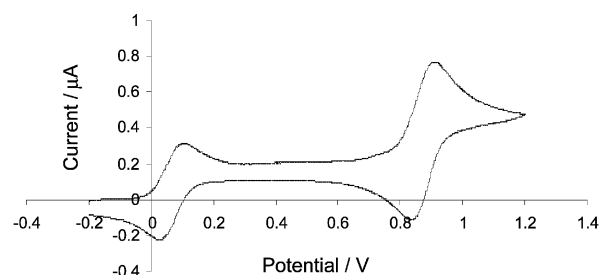


**Fig. 5** Voltammetric oxidation of  $[(bpy)_2Ru(pbimC_3)](PF_6)_2$  (1 mM) complex in acetonitrile at a platinum electrode. Ferrocene standard added. Scan rate 100  $mV s^{-1}$ .

trode is  $[(bpy)_2Ru(pbimC_4)](PF_6)_2 > [(bpy)_2Ru(pbimC_3)](PF_6)_2$  ( $\approx [(bpy)_2Ru(pbimH)](PF_6)_2 > [(bpy)_2Ru(pbimC_2)](PF_6)_2$ ). This is because of the electron withdrawing nature of the carboxylic acid group  $-CH_2CO_2H$ . The electron density of the metal center is lower than that of  $[(bpy)_2Ru(pbimH)](PF_6)_2$  and thus it is more difficult to oxidize. For complex  $[(bpy)_2Ru(pbimC_4)](PF_6)_2$ , however, because the carboxylic group is further away,  $-CH_2CH_2CH_2CO_2H$  becomes electron donating rather than withdrawing, which increases the electron density of the metal center. A similar observation was reported for the effect of alkylation of the related tridentate bis(benzimidazole) pyridine (dbip) ligand.<sup>28</sup> The redox potentials are not so different from that of the pbimH complex. In **2b** the  $CO_2H$  groups is closest to the pbim ring and this has the effect of raising the potential. For  $[Ru(bpy-(CH_2)_3CO_2H)(dmbpy)_2]^{3+}$  the  $Ru(III/II)$  couple was shifted 60 mV more cathodic than  $[Ru(bpy-CO_2H)(dmbpy)_2]$ .<sup>27</sup> As the chain-length increases the potential falls, as expected for

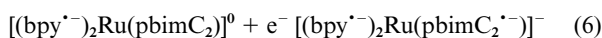
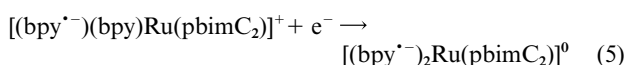
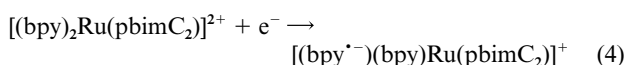
**Table 4** Voltammetric data obtained for the reduction of the ruthenium 2-(2'-pyridyl)benzimidazole complexes (1 mM) in acetonitrile at a platinum electrode. The scan rate was 100 mV s<sup>-1</sup>

Compound	Redox potential/V (vs. Fc/Fc <sup>+</sup> )					
	$E_p^{\text{red}} (E_p^{\text{ox}})$	$E_{1/2}$	$E_p^{\text{red}} (E_p^{\text{ox}})$	$E_{1/2}$	$E_p^{\text{red}} (E_p^{\text{ox}})$	$E_{1/2}$
[(bpy) <sub>2</sub> Ru(pbimH)](PF <sub>6</sub> ) <sub>2</sub>	-1.617 (—)	—	-1.901 (-1.815)	-1.853	-2.133 (-2.061)	-2.097
[(bpy) <sub>2</sub> Ru(pbimC <sub>2</sub> )](PF <sub>6</sub> ) <sub>2</sub>	-1.820 (-1.744)	-1.782	-2.030 (-1.950)	-1.990	-2.292 (-2.222)	-2.257
[(bpy) <sub>2</sub> Ru(pbimC <sub>3</sub> )](PF <sub>6</sub> ) <sub>2</sub>	-1.808 (-1.730)	-1.701	-2.006 (-1.926)	-1.898	-2.254 (-2.180)	-2.217
[(bpy) <sub>2</sub> Ru(pbimC <sub>4</sub> )](PF <sub>6</sub> ) <sub>2</sub>	-1.805 (-1.731)	-1.768	-2.003 (-1.933)	-1.968	-2.259 (-2.179)	-2.219

the electron-donating effect of an alkyl group. For the related tridentate bis(benzimidazole) pyridine (dbip) ligand the shift was 60 mV cathodic.<sup>28</sup>

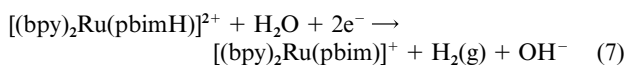


The alkylated pbim complexes display three one-electron reduction waves (Table 4; CV shown for the pbimC<sub>2</sub> complex in Fig. 6). These are assigned to the reduction of each of the two bpy ligands, followed by the reduction of the pbim ligands:



The potential for the reduction of the pbim ligand accords with the expected trends in the ligand π\* energies. In agreement with this assignment, the third reduction process shows the most variation between the complexes; that of [Ru(bpy)<sub>2</sub>(pbimC<sub>2</sub>)](PF<sub>6</sub>)<sub>2</sub> is slightly more negative because of the electron withdrawing effect from the carboxylic acid group. In comparison, the complex [RuL<sub>2</sub>]<sup>2+</sup>, L = 2,6-bis(benzimidazole)pyridine, does not have such straightforward electrochemistry, showing one irreversible wave at -1.70 V vs. Ag/Ag<sup>+</sup>.<sup>28</sup>

Somewhat different behaviour is observed for the pbimH complex (Fig. 6). Only two reversible waves are observed, and these are preceded by an irreversible reduction. None of these waves were reported in the original work by Haga, although in a footnote it was claimed that additional waves at in this region disappeared when dry alumina was added to the cell.<sup>29</sup> We propose that the irreversible reduction is due to the reduction of released protons from the pbim ligand (overall reaction shown in eqn. (7)):



This explanation is related to that proposed for similar cyclic voltammetry behaviour noted for RuN<sub>3</sub> (1) by Wolfbauer *et al.*<sup>30</sup> They showed that the proton reduction reaction was highly dependent on the nature of the electrode. If gold or carbon is used the proton reduction is suppressed to some extent as shown in Fig. 7. Deprotonation of the pbimH ligand cathodically shifts the redox potentials of the bpy reduction by about 100 mV. The pbim ligand reduction is shifted by about 350 mV compared to the alkylated ligand complexes to -2.6 V. This region is close to the solvent reduction and the wave appears as a double wave possibly overlapping with a metal-based reduction process.

### Surface attachment chemistry

In solar cells, the carboxylic acid or ester functional groups are necessary for achieving a high surface coverage, apart from the porosity of the nanocrystalline semiconductor that was used for

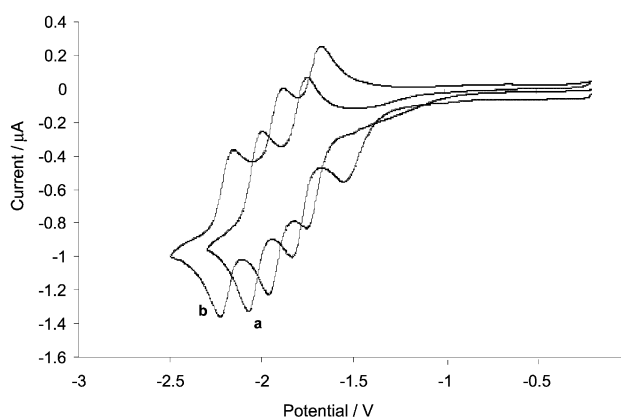


**Fig. 6** Reduction of [(bpy)<sub>2</sub>Ru(pbimH)](PF<sub>6</sub>)<sub>2</sub> (trace a), [(bpy)<sub>2</sub>Ru(pbimC<sub>2</sub>)](PF<sub>6</sub>)<sub>2</sub> (trace b) (1 mM) in acetonitrile at a platinum electrode. Scan rate 100 mV s<sup>-1</sup>.

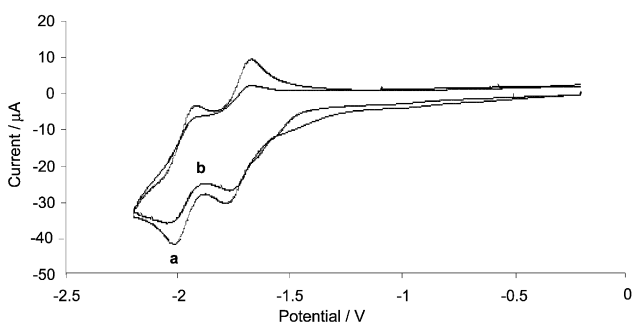


**Fig. 7** Reduction of [(bpy)<sub>2</sub>Ru(pbimH)](PF<sub>6</sub>)<sub>2</sub> (1 mM) in acetonitrile at carbon (trace a) and Au (trace b) electrodes at 100 mV s<sup>-1</sup>.

the electrode. The analogous sensitizers that do not possess such groups display surface coverages that are at least an order of magnitude lower.<sup>25</sup> All of the studied complexes adsorbed strongly onto oxide surfaces with the exception of the pbimH parent complex.

**(1) IR and UV-Vis spectroscopy.** The infrared spectra of the TiO<sub>2</sub> semiconductor and [(bpy)<sub>2</sub>Ru(pbimC<sub>2</sub>)](PF<sub>6</sub>)<sub>2</sub> absorbed onto the TiO<sub>2</sub> semiconductor showed that the asymmetric stretching ν(CO<sub>2</sub><sup>-</sup>) at 1605 cm<sup>-1</sup> indicated the formation of the ester bond between the carboxylic and the TiO<sub>2</sub> hydroxyl groups. Goodenough *et al* suggested that a dehydrative coupling reaction between the sensitizer, 4,4'-dicarboxyl-2,2'-bipyridine, for example, and the surface hydroxyl groups on rutile TiO<sub>2</sub> would yield an ester linkage on the surface with enhanced electronic coupling between the π\* orbital of the bipyridine ring and the Ti 3d orbital manifold of the semiconductor.<sup>31</sup> The UV-Vis spectrum of the adsorbed complexes were virtually identical to the solution spectrum. Despite this it has been shown in other work that the photocurrent action of sensitizers may reveal a significant red shift upon surface attachment, consistent with surface stabilization of the MLCT excited state.<sup>1,32</sup>

**(2) Cyclic voltammetry.** Cyclic voltammograms of the oxidation of [(bpy)<sub>2</sub>Ru(pbim)](PF<sub>6</sub>)<sub>2</sub> on a TiO<sub>2</sub> semiconductor

**Table 5** Lifetimes (ns) of the dye-sensitizers obtained from both free solution and onto TiO<sub>2</sub> films ( $I_v \approx 6.0 \times 10^{-5}$  mol cm<sup>-2</sup>). Errors  $\pm 15\%$ , or greater at the shorter times

Compound	MeCN solution			ZrO <sub>2</sub> films			TiO <sub>2</sub> films		
	$\tau_1$	$\tau_2$	$\tau_{av}$	$\tau_1$	$\tau_2$	$\tau_{av}$	$\tau_1$	$\tau_2$	$\tau_{av}$
[(bpy) <sub>2</sub> Ru(pbimC <sub>2</sub> )](PF <sub>6</sub> ) <sub>2</sub>	224	27.6	148	367	81	299	88.6	11.5	45.3
[(bpy) <sub>2</sub> Ru(pbimC <sub>3</sub> )](PF <sub>6</sub> ) <sub>2</sub>	206	18.2	188	388	102	308	138	16.3	66.1
[(bpy) <sub>2</sub> Ru(pbimC <sub>4</sub> )](PF <sub>6</sub> ) <sub>2</sub>	297	180	237	386	147	284	109	11.1	46.1

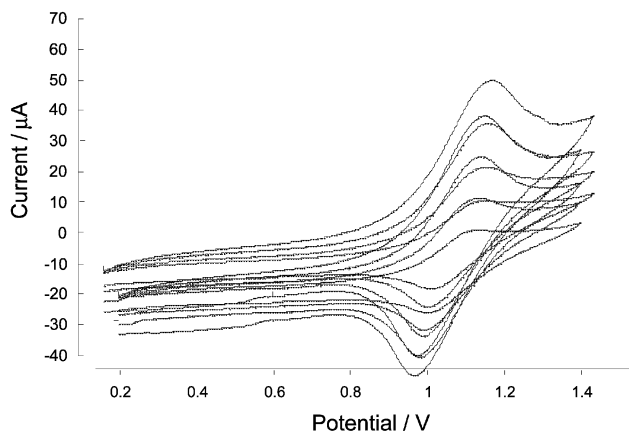


**Fig. 8** Cyclic voltammograms of [(bpy)<sub>2</sub>Ru(pbimC<sub>2</sub>)](PF<sub>6</sub>)<sub>2</sub> adsorbed onto a TiO<sub>2</sub> semiconductor electrode in 0.1 M <sup>t</sup>Bu<sub>4</sub>NPF<sub>6</sub> CH<sub>2</sub>Cl<sub>2</sub> solution. The data were recorded at scan rates of 20, 40, 80 and 100 mV s<sup>-1</sup>.

electrode are shown in Fig. 8. The complex [(bpy)<sub>2</sub>Ru(pbimC<sub>2</sub>)](PF<sub>6</sub>)<sub>2</sub> displays a reversible Ru(III/II) redox process by cyclic voltammetry both in fluid solution and when anchored to the nanocrystalline TiO<sub>2</sub> film. The peak-to-peak separation for the surface-bound sensitizer is almost twice that in the free solution, for example 186 mV for anchored dye and 80 mV in solution at 100 mV s<sup>-1</sup>. The redox process is therefore quasi-reversible. The redox potential, however, decreased from 808 to 708 mV. This means that, once anchored to the semiconductor, the dye-sensitizer became more easily oxidized. The area under the peak gives the surface coverage of electroactive complex ( $\Gamma_e$ , eqn. (8)).

$$\Gamma_e = \frac{Q}{nFS} \quad (8)$$

$$\Gamma_v = \frac{A}{\varepsilon} \quad (9)$$

where  $Q$  is the charge,  $n$  is the number of electrons transferred,  $F$  is the Faraday constant,  $S$  is the area of the electrode;  $A$  is the absorbance at the peak maximum and  $\varepsilon$  is the extinction coefficient. Compared with that calculated from the UV-Vis absorbance ( $\Gamma_v$ , eqn. (9)), more than 90% of ruthenium centres are redox-inactive. As suggested previously<sup>33</sup> this inactivity probably rules out lateral redox hopping between complexes on the surface of TiO<sub>2</sub>. However, a recent paper has found much higher electroactivity in amine dye coatings, indicating lateral charge transfer.<sup>34</sup>

#### Time-resolved photoluminescence spectroscopy

Normalized photoluminescence quenching decays of the dye-sensitizer [(bpy)<sub>2</sub>Ru(pbimC<sub>2</sub>)](PF<sub>6</sub>)<sub>2</sub> both in free solution and on ZrO<sub>2</sub> and TiO<sub>2</sub> films are shown in Fig. 9. Data from experiments on the other dye-sensitizer are collected in Table 5. The lifetimes were obtained from the second-order exponential decay fit of the spectra. On ZrO<sub>2</sub> films, no electron transfer occurs because the energy level of the conduction band is higher than that of the excited state of the dye-sensitizer.<sup>35</sup>

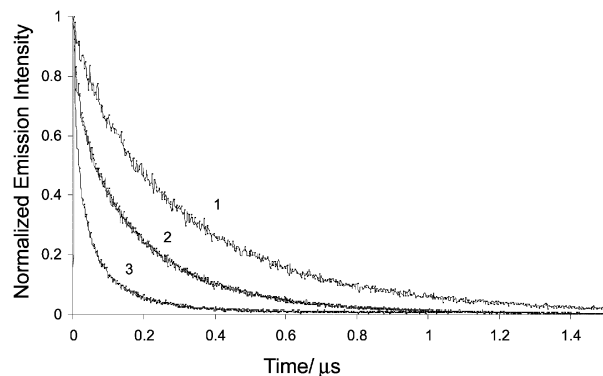


**Fig. 9** Normalized time-resolved photoluminescence spectra recorded at 650 nm after pulsed at 400 nm excitation of [(bpy)<sub>2</sub>Ru(pbimC<sub>2</sub>)](PF<sub>6</sub>)<sub>2</sub> on (1) ZrO<sub>2</sub>, (2) in free solution and (3) on TiO<sub>2</sub> films in acetonitrile solution.

Much reduced lifetimes were observed on the TiO<sub>2</sub> semiconductor electrode due to electron injection. The same phenomena were observed for pbimC<sub>3</sub> and pbimC<sub>4</sub> complexes. Our results are comparable with those of [Ru(bpy)<sub>2</sub>(4,4'-(PO<sub>3</sub>H<sub>2</sub>)<sub>2</sub>-bpy)](PF<sub>6</sub>)<sub>2</sub> tested on TiO<sub>2</sub> film (27 ns) and on ZrO<sub>2</sub> film (960 ns).<sup>33</sup> The shorter lifetimes detected on TiO<sub>2</sub> are consistent with efficient charge injection, and it is possible to obtain a charge injection rate from the difference in the reciprocal lifetimes on TiO<sub>2</sub> and ZrO<sub>2</sub><sup>36</sup> but the errors were rather large at these short timescales close to the limit of the instrument and no clear trends were discerned from these data. In addition, the traces may be composites of several kinetic processes such as: (1) luminescence decay from complexes adsorbed at multiple sites; (2) luminescence from impurities present in the system (e.g. released ligands); and (3) charge injection from molecules not directly attached to the surface. Despite these *caveats*, the data suggests that charge injection is possible using our complexes, and the behaviour as solar cell sensitizers should resemble that of other pendant chain complexes such as [(bmp)<sub>2</sub>RuL]<sup>2+</sup> (bmp = 4,4'-dimethyl-2,2'-bipyridyl, L = 4-(3-carboxypropyl)-2,2'-bipyridyl).<sup>27</sup> These complexes have similar redox potentials and so the driving force for the back reaction and the reaction with iodide should be comparable.

#### Solar energy conversion using the complexes

Disappointingly, the IPCE values that we observed for Grätzel-type solar cells using the pbim complexes as sensitizers are very small, <1%. The sensitivity of our equipment at this level was not sufficient to make a detailed comparison of the complexes. The open-circuit voltage ( $V_{oc}$ ) and short-circuit current ( $I_{sc}$ ) tested under direct sunlight (AM 1.5) of the solar cells based on the dye-sensitizer pbim derivative complexes are shown in Table 6. The open-circuit voltage is known to be directly related to the rate of charge injection relative to the rates of removal of the injected electron (e.g. by the back reaction).<sup>15</sup> The  $V_{oc}$  data clearly fall as: [(bpy)<sub>2</sub>Ru(pbimC<sub>2</sub>)](PF<sub>6</sub>)<sub>2</sub> > [(bpy)<sub>2</sub>Ru(pbimC<sub>3</sub>)](PF<sub>6</sub>)<sub>2</sub> > [(bpy)<sub>2</sub>Ru(pbimC<sub>4</sub>)](PF<sub>6</sub>)<sub>2</sub>, the expected trend as the chain-length increases. It appears that the apparently efficient charge injection rates suggested by the photoluminescence data are in fact slower than standard dyes and do not compete well with intramolecular deactivation processes of the excited state.

**Table 6** Data from the solar cell of the pbim derivatives of ruthenium complexes tested under direct sunlight ( $G_{\text{v}} \approx 6.0 \times 10^{-5} \text{ mol cm}^{-2}$ )

Compound	$V_{\text{oc}}/\text{mV}$	$I_{\text{sc}}/\mu\text{A}$
$[(\text{bpy})_2\text{Ru}(\text{pbimC}_2)](\text{PF}_6)_2$	273	96
$[(\text{bpy})_2\text{Ru}(\text{pbimC}_3)](\text{PF}_6)_2$	177	60
$[(\text{bpy})_2\text{Ru}(\text{pbimC}_4)](\text{PF}_6)_2$	135	47

Further experiments such as time-resolved transient absorption measurements on the ps timescale will be necessary to confirm this point.

Low IPCE values have also been observed for sensitizers with pendant linkage groups; for example, modification of  $\text{RuN}_3$  by inserting a phenyl group between the bpy and the carboxylic acid group was found to decrease the IPCE from over 80% to only 8%,<sup>37</sup> while a propyl group led to a *ca.* 50% decrease.<sup>27</sup> Lowering of the IPCE to 2% or less was observed using proline-type anchors of length 14–16 Å instead of the usual carboxylated bpy ligands.<sup>33</sup> In contrast, for a series of merocyanine dye-sensitizers the efficiency increased as the chain length increased to 18–20 carbon atoms. It was proposed that the back electron transfer reaction was dominant in this case.<sup>38</sup> An interesting study was carried out on  $[\text{ReCl}(\text{CO})_3(\text{bpy}-(\text{CH}_2)_2\text{CO}_2\text{H})]$  sensitizers.<sup>39</sup> It was shown that inserting the first  $\text{CH}_2$  group led to a 200-fold drop—much greater than predicted from Marcus theory of electron-transfer distance dependence. Thereafter, however, increasing the chain length decreased the rate in line with theory. A similar trend was observed for Fe sensitizers.<sup>40</sup>

A further, perhaps more serious problem with the pbim complexes is that the  $\pi^*$  energy level of the pbim ligand is much higher than that of the other bpy ligands. Evidence for this lies in the assignment of the first two reduction potentials as being bpy based. This means that in the excited state the electron resides on the bpy ligand, rather than the pbim. As a consequence the electron is very far from the anchoring point to the surface of the  $\text{TiO}_2$ . It has been shown that this is deleterious to the IPCE; for example, in terpy/biquinoline mixed ligand sensitizers the IPCE falls from 75.6% to 1.74%.<sup>37</sup> The use of alternative ligands to bipyridine or the preparation of homoleptic pbim complexes may solve this problem.

## Conclusions

The new carboxylated pbim complexes display well-resolved NMR spectra which can be fully assigned by 2D NMR spectroscopy. The pbimH complex electrochemistry has been reinvestigated and evidence was presented for reduction of the deprotonated ligand. The carboxylated pbim complexes show good electrochemical reversibility, with slightly more positive redox potentials than the pbimH parent complex. In general, the spectroscopic (light-harvesting) and electrochemical properties of the carboxylated complexes (relating to electron collection efficiency) were very similar. Hence, any difference in solar-cell sensitization performance must be due to changes in the length of the spacer. Unfortunately, the higher  $\pi^*$  energy level of the pbim ligand means that the electron in the MLCT excited state resides on bpy, well away from the anchoring point. Consequently, the IPCE values are too low to differentiate between the complexes, but a fall in the open-circuit potential as the chain length increases was observed.

## Acknowledgements

We thank Dr D. T. Richens (School of Chemistry), Dr Bruce Sinclair (School of Physics) and Dr Ebinazar Namdas (Organic Semiconductor Centre) and the CVCP for an ORS scholarship to H. Y. We thank the Carnegie Fund and the University

St. Andrews for funding Miss Gemma Holliday who helped with the electrochemical analysis.

## References

- 1 M. K. Nazeeruddin, A. Kay, I. Rodicio, R. Humphry-Baker, E. Muller, P. Liska, N. Vlachopoulos and M. Grätzel, *J. Am. Chem. Soc.*, 1993, **115**, 6382–6390.
- 2 K. Kalyanasundaram and M. Grätzel, *Coord. Chem. Rev.*, 1998, **177**, 347–414.
- 3 J. J. Kelly and D. Vanmaekelbergh, *Electrochim. Acta*, 1998, **43**, 2773–2780.
- 4 J. E. Moser, P. Bonnote and M. Grätzel, *Coord. Chem. Rev.*, 1998, **171**, 245–250.
- 5 L. M. Peter, E. A. Ponomarev, G. Franco and N. J. Shaw, *Electrochim. Acta*, 1999, **45**, 549–560.
- 6 C. A. Bignozzi, R. Argazzi and C. J. Kleverlaan, *Chem. Soc. Rev.*, 2000, **29**, 87–96.
- 7 C. G. Garcia, J. F. de Lima and N. Y. M. Iha, *Coord. Chem. Rev.*, 2000, **196**, 219–247.
- 8 C. A. Kelly and G. J. Meyer, *Coord. Chem. Rev.*, 2001, **211**, 295–315.
- 9 A. Hagfeldt and M. Grätzel, *Chem. Rev.*, 1995, **95**, 49–68.
- 10 A. Hagfeldt and M. Grätzel, *Acc. Chem. Res.*, 2000, **33**, 269–277.
- 11 J. M. Stipkala, F. N. Castellano, T. A. Heimer, C. A. Kelly, K. J. T. Livi and G. J. Meyer, *Chem. Mater.*, 1997, **9**, 2341–2353.
- 12 B. O'Regan and M. Grätzel, *Nature*, 1991, **353**, 737–740.
- 13 A. Zaban, S. Ferrere and B. A. Gregg, *J. Phys. Chem. B*, 1998, **102**, 452–460.
- 14 M. K. Nazeeruddin, P. Pechy and M. Grätzel, *Chem. Commun.*, 1997, 1705–1706.
- 15 R. Argazzi, C. A. Bignozzi, T. A. Heimer, F. N. Castellano and G. J. Meyer, *J. Am. Chem. Soc.*, 1995, **117**, 11815–11816.
- 16 A. Yoshimura, K. Nozaki, N. Ikeda and T. Ohno, *Bull. Chem. Soc. Jpn.*, 1996, **69**, 2791–2799.
- 17 S. A. Thomson, J. A. Josey, R. Cadilla, M. D. Gaul, C. F. Hassman, M. J. Luzzio, A. J. Pipe, K. L. Reed, D. J. Ricca, R. W. Wiethe and S. A. Noble, *Tetrahedron*, 1995, **51**, 6179–6194.
- 18 M. K. Nazeeruddin, E. Muller, R. Humphry-Baker, N. Vlachopoulos and M. Grätzel, *J. Chem. Soc., Dalton Trans.*, 1997, 4571–4578.
- 19 O. Kohle, S. Ruile and M. Grätzel, *Inorg. Chem.*, 1996, **35**, 4779–4787.
- 20 S. Ruile, O. Kohle, P. Pechy and M. Grätzel, *Inorg. Chim. Acta*, 1997, **261**, 129–140.
- 21 R. K. Boggess and R. B. Martin, *Inorg. Chem.*, 1974, **13**, 1525.
- 22 M. R. Grimmett, in *Comprehensive Heterocyclic Chemistry*, A. R. Katritzky and C. W. Rees, eds., 1979, pp. 382–390.
- 23 K. H. Mayer, *Synthesis*, 1975, 673.
- 24 M. A. Haga, *Inorg. Chim. Acta*, 1983, **75**, 29.
- 25 P. Qu and G. J. Meyer, *Langmuir*, 2001, **17**, 6720–6728.
- 26 Y. J. Hou, P. H. Xie, B. W. Zhang, Y. Cao, X. R. Xiao and W. B. Wang, *Inorg. Chem.*, 1999, **38**, 6320.
- 27 T. A. Heimer, S. T. Darcangelis, F. Farzad, J. M. Stipkala and G. J. Meyer, *Inorg. Chem.*, 1996, **35**, 5319–5324.
- 28 X. M. Xiao, M. A. Haga, T. Matsumurainoue, Y. Ru, A. W. Addison and K. Kano, *J. Chem. Soc., Dalton Trans.*, 1993, 2477–2484.
- 29 M. A. Haga and A. Tsunemitsu, *Inorg. Chim. Acta*, 1989, **164**, 137.
- 30 G. Wolfbauer, A. M. Bond, G. B. Deacon, D. MacFarlane and L. Spiccia, *J. Am. Chem. Soc.*, 2000, **122**, 130.
- 31 S. Anderson, E. C. Constable, M. P. Dare-Edwards, J. B. Goodenough, A. Hamnett, K. R. Seddon and R. D. Wright, *Nature*, 1979, **280**, 571.
- 32 D. A. Gulino and H. G. Drickamer, *J. Phys. Chem.*, 1984, **88**, 1173.
- 33 S. A. Trammell, J. A. Moss, J. C. Yang, B. M. Nakhle, C. A. Slate, F. Odobel, M. Sykora, B. W. Erickson and T. J. Meyer, *Inorg. Chem.*, 1999, **38**, 3665.
- 34 P. Bonhote, E. Gogniat, S. Tingry, C. Barbe, N. Vlachopoulos, F. Lenzmann, P. Comte and M. Grätzel, *J. Phys. Chem. B*, 1998, **102**, 1498.
- 35 Y. Tachibana, J. E. Moser, M. Grätzel, D. R. Klug and J. R. Durrant, *J. Phys. Chem.*, 1996, **100**, 20056.
- 36 R. Argazzi, C. A. Bignozzi, T. A. Heimer, F. N. Castellano and G. J. Meyer, *Inorg. Chem.*, 1994, **33**, 5741.
- 37 B. W. Jing, H. Zhang, M. H. Zhang, Z. H. Lu and T. Shen, *J. Mater. Chem.*, 1998, **8**, 2055.
- 38 K. Sayama, S. Tsukagoshi, K. Hara, Y. Ohga, A. Shinpou, Y. Abe, S. Suga and H. Arakawa, *J. Phys. Chem. B*, 2002, **106**, 1363.
- 39 J. B. Asbury, E. C. Hao, Y. Q. Wang and T. Q. Lian, *J. Phys. Chem. B*, 2000, **104**, 11957.
- 40 S. Ferrere, *Chem. Mater.*, 2000, **12**, 1083.